J Mater Sci (2011) 46:183–187
DOI 10.1007/s10853-010-4906-5

UV laser ablation of parylene films from gold substrates

O. R. Musaev · P. Scott · J. M. Wrobel · J. A. Wolf · M. B. Kruger

Received: 2 July 2010 / Accepted: 6 September 2010 / Published online: 29 September 2010

Abstract Parylene coatings on gold substrates were removed by laser ablation using 248-nm light from an excimer laser. Each sample was processed by a different number of pulses in one of three environments: air at atmospheric pressure, nitrogen at atmospheric pressure, and vacuum. The laser-induced craters were analyzed by optical microscopy and X-ray photoelectron spectroscopy. Multi-pulse ablation thresholds of gold and parylene were determined.

Introduction

Parylene is an organic polymer that has a variety of technological applications. For example, it is used as a protective layer in printed circuit boards, as a flexible substrate for microwave integrated circuits and as a biocompatible coating for microelectrodes in neural science [1–4]. High biocompatibility makes parylene a valuable material for biomedical engineering. Selective parylene removal is required for various applications, in particular, for BioMEMS and microfluidic devices [2]. Removal of parylene was developed based on photolithography and dry etching of parylene films on silicon substrates [2].

There are currently a variety of methods employed to remove parylene. Chemical removal is problematic due to the inert nature of parylene [5]. Dry etching processes are currently considered the most suitable for batch processing of parylene structures. These methods include plasma etching, ion reactive etching, and deep reactive etching [5]. However, plasma etching is complex and other simpler techniques would be desirable. Laser-assisted selective removal of parylene promises to be an efficient approach.

Beginning in the early 1980s, laser ablation of polymers has attracted attention [6]. It has become an area of interest in various fields including the microelectronics industry, bioengineering, and chemistry [7]. Laser ablation of parylene was performed as early as 1991 and has more recently been used in developing high aspect ratio (~ 100) three-dimensional (3D) multi-electrode MEMS arrays and to remove parylene from the tips of biomedical microelectrodes [3, 8–10]. High aspect ratio 3D multi-electrode arrays were fabricated using laser-assisted selective removal of micron thick parylene film from a copper surface [9]. Platinum micro-electrodes for neural research were fabricated by laser-assisted removal of parylene from platinum tips [3, 11]. In MEMS technology, fabrication of 3D metallic structures in high aspect ratio cavities is a challenge. Standard approaches based on photolithography provide insufficient resolution and have restrictions on aspect ratio. Laser-assisted fabrication of thick electroplated metallic patterns in high aspect ratio cavities is a promising approach [10].

O. R. Musaev · P. Scott · J. M. Wrobel (✉) · M. B. Kruger
Department of Physics, University of Missouri-Kansas City, Kansas City, MO 64110, USA
e-mail: wrobelj@umkc.edu

J. A. Wolf
National Nuclear Security Administration's Kansas City Plant, Kansas City, MO 64141, USA

For fabrication purposes, it is often necessary to remove a thin layer of parylene ($\sim$10 μm) from a metal surface without damaging it. It is important to understand how the etching of parylene depends on parameters of the process, such as the surrounding medium, fluence, wavelength, and number pulses. In this study, we investigated laser ablation of parylene from gold surfaces. The purpose of this study was to establish conditions for efficient removal of parylene while preserving the surface of the underlying metal. The effects of ablation environments, and combination of fluences and number of pulses were determined.

Experimental

The samples studied were either thin films of bare gold (28 μm thick) or gold coated with a 8-11-μm layer of parylene-C [poly(monochloro-*p*-xylylene)]. All samples were prepared at Honeywell Federal Manufacturing & Technologies. Parylene-C has the structure shown in Fig. 1. A Lambda Physics KrF excimer laser, model LPX-210, operating at 248 nm with pulse duration of 20 ns (according to specifications), was used for ablation of gold and parylene. Homogenization of the light used for ablation was achieved by expansion of the laser beam and placing a circular aperture at the beam's center. A small fraction ($\sim$1%) of the radiation coming from the laser was transmitted through the hole in the aperture. A three-element converging lens system focused the light to a 0.5-mm diameter circle on the sample's surface. The pulse energy was measured using an Ophir energy/power meter, and the fluence was determined from this measurement and the area of the processed spot. The fluence in the processes was varied between 300 and 800 mJ/cm^2. Samples were placed in a small vacuum chamber and processed in air (room temperature, humidity $\sim$35%), nitrogen, and vacuum ($\sim 10^{-2}$ Torr). For samples processed in air, the chamber was opened to air. For samples processed in nitrogen, the chamber was purged with nitrogen during processing. A mechanical pump was used to evacuate the chamber for samples processed in vacuum.

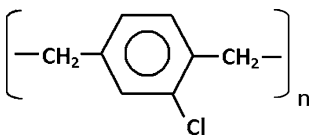

Fig. 1 Chemical structure of parylene-C

For determination of the ablation threshold and processing rates of both parylene and gold, depths of the ablation craters were optically measured and microphotographs of the laser-processed craters were taken. For cases of visible carbon deposits, the surface was first cleaned in an ultrasonic bath filled with distilled water before measurements were made. Chemical analysis of the processed spots with X-ray photoelectron spectroscopy (XPS) was used to probe for the presence of gold, carbon, and chlorine. An optical microscope with a high magnification objective (100×) was used to measure the depths of the craters in the gold and parylene surfaces. This was done by focusing on the ablated and unablated portions of the sample.

Results and discussion

The effect of 248-nm laser radiation on an uncoated gold surface was investigated. In Fig. 2, the damage to the gold surface for four different fluences is shown. In each case, the surface was exposed to 300 laser pulses and the process was carried out in air. Fluence values used here were just above the multi-pulse ablation threshold of gold. One should recognize that the fluences used are much lower than the single-pulse ablation threshold, which is about 2 J/cm^2 [12].

An optical microscope was used to measure the depth of the craters. The obtained experimental dependence of crater depth for 300 pulses on fluence is plotted in Fig. 3. The best linear fit and the extrapolation of the relationship to low fluences yield the ablation threshold for gold under these conditions to be about 255 mJ/cm^2.

In order to investigate the effect of accidental exposure of gold to laser radiation after removal of parylene, the effect of the number of pulses at the fluence comparable to that used for ablation of parylene was carried out. As shown in Fig. 4, the rate at which gold was ablated was not constant but varied with the number of pulses. The etched

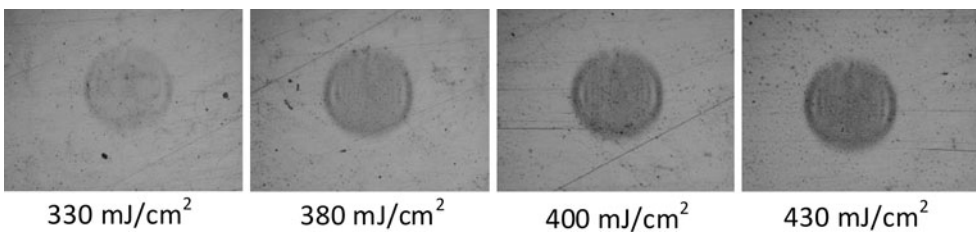

Fig. 2 Optical images of the surface of gold after illumination with 300 pulses at the indicated fluences. Ablation took place in air. The diameter of the holes is 0.5 mm

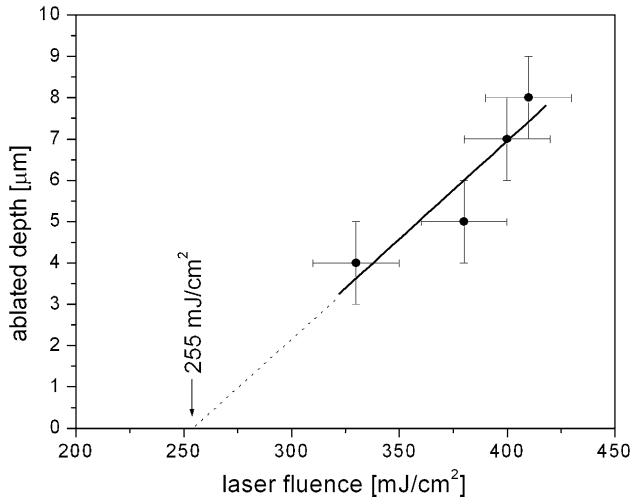

Fig. 3 Determination of the ablation threshold of gold in air at 248 nm for 300 pulses

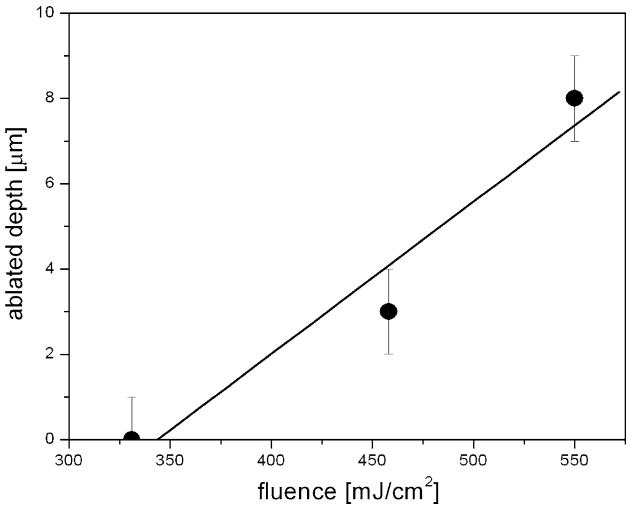

Fig. 5 Determination of the 10-pulse ablation threshold of parylene in air at 248 nm

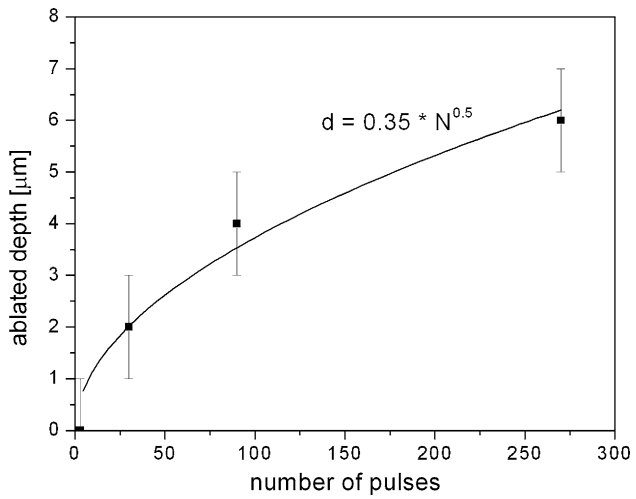

Fig. 4 Depth of gold ablated at 248 nm versus the number of pulses. The fluence was 310 mJ/cm^2

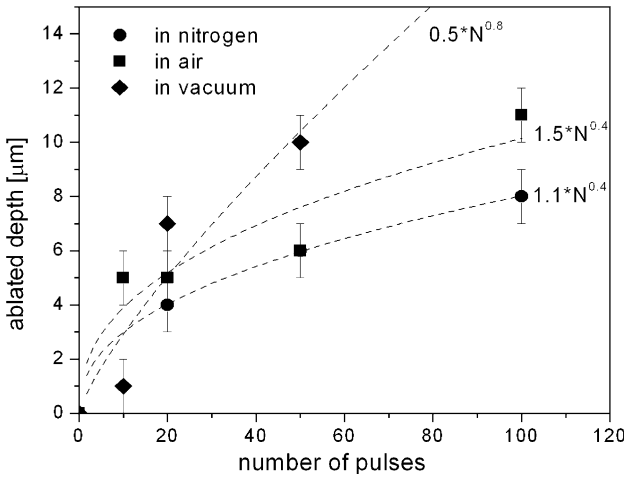

Fig. 6 Depth of parylene ablated by 248 nm light in nitrogen (8-μm thick parylene film), air (11-μm thick parylene film), and vacuum (10-μm thick parylene film) versus the number of pulses. The laser fluence was 330 mJ/cm^2

depth is a power function of the number of pulses, with the exponent of 0.5.

Previously, a KrF excimer laser was used to study ablation of parylene from gold films at fluences in the range 6.7–26.7 mJ/cm^2 [10]. In that research, an approximately linear dependence of ablation depth on the number of pulses (200–1000) was observed. In this study, the ablation of parylene films from gold substrates was performed at fluences between 330 and 550 mJ/cm^2. In Fig. 5, the depth of ablation by 10 pulses for different fluences is depicted. From this, the ablation threshold at 10 pulses is estimated to be 340 mJ/cm^2. This is in good agreement with an estimation that can be obtained from previously published data [8].

The 10-pulse ablation threshold of parylene is greater than the 300-pulse ablation threshold of gold. During processing, the thickness of the film decreases, increasing the illumination of the substrate, which increases the possibility of damage to the substrate. Thus, the complete removal of parylene may result in some damage to the gold substrate. This implies that adaptive control of the laser fluence may be the method of choice for parylene film removal. Thus, the goal of adaptive control is to decrease fluence with pulse number, in such a way as to maximize film removal while leaving the substrate undamaged.

In Fig. 6, the depth of parylene removed at a fluence of 330 mJ/cm^2 is plotted versus the number of pulses for three environments: nitrogen, air, and vacuum. The ablated depth

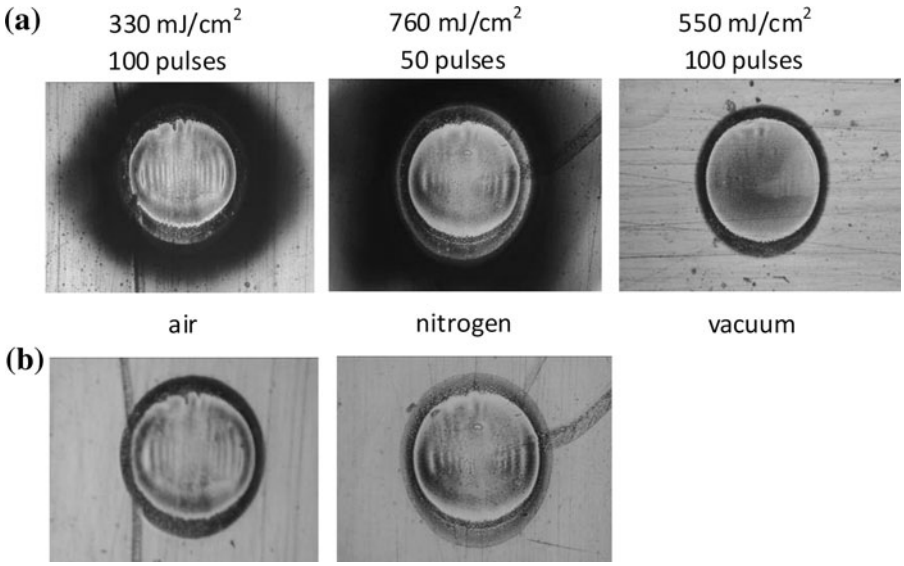

Fig. 7 Optical microscope images of holes ablated in 8–11 μm parylene-C layers on gold: **a** before cleaning; **b** after 3 min in an ultrasonic bath. The diameter of the holes is 0.5 mm

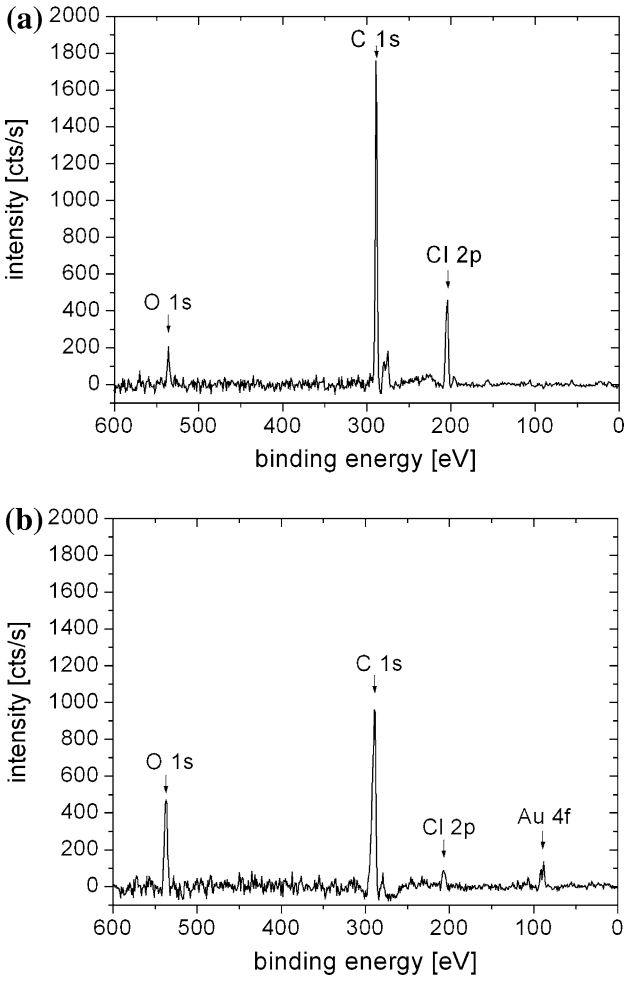

Fig. 8 X-ray photoemission spectra (baseline subtracted) from **a** a parylene film and **b** an etched crater

is not directly proportional to the number of pulses. As the process continues the ablation rate decreases. Similar to the case of gold, the amount of ablated parylene, as a function of the number of pulses, follows a power law. In both nitrogen and air, the rates are comparable, however, a significantly higher rate is observed in vacuum. The decrease of the ablation rate with the number of pulses can be related to the change of morphology or material modification and chemical composition change of the irradiated area. For example, in the ablation of polyimide, the ablation rate strongly decreases with the number of pulses [13]. This occurs for two reasons: roughness increases with the number of pulses, which causes a decrease of effective fluence, and carbonization of the material, which alters the ablation conditions. The same effects, increased roughness and carbonization, occur during ablation of parylene.

Optical images of ablated craters in parylene on gold, obtained under different conditions, are presented in Fig. 7. Ablation in air and nitrogen resulted in obvious deposits of carbon in the vicinity of the etched craters. As seen in the top row of the figure, the size of the carbon deposits extends up to 0.5 mm from the edge of the craters. An attempt to remove this carbon by placing the samples in distilled water in an ultrasonic bath was effective as can be seen in Fig. 7b.

From Fig. 7a, it is clear that carbon is not deposited on the sample during ablation in vacuum. This can be explained by uninhibited expansion of the plasma plume into vacuum. Carbon particles move with the flow and are not deposited on the sample.

Chemical processes taking place during ablation were investigated using XPS. Craters etched under different

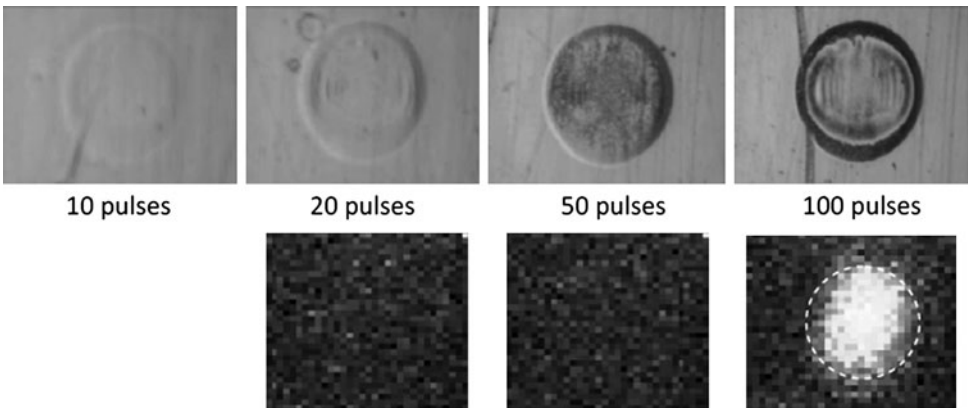

Fig. 9 Evolution of the morphology and chemical composition of the ablated surface with the number of pulses. The parylene film was 11-μm thick and the laser had a fluence of 330 mJ/cm^2

conditions were studied. As seen in Fig. 8a, oxygen 1s, carbon 1s, and chlorine 2p lines have been detected in the unprocessed regions of the samples. Since oxygen is not present in any of the parylene compounds, it is probably present in the form of adsorbed water. In the XPS spectrum from an etched crater, shown in Fig. 8b, the 4f line of gold appears. It is possible that a trace of parylene is observed in the crater, as evidenced by the low intensity Cl 2p line.

The evolution of optical images and XPS maps of craters as a function of the number of laser pulses is presented in Fig. 9. The top row consists of optical micrographs and the bottom row shows the corresponding maps of the XPS intensity of the 4f gold line. The non-uniform distribution of the gold line intensity suggests that the gold surface is not completely clean.

Conclusion

Laser ablation of gold in air and parylene films on gold, in air, vacuum, and nitrogen gas was performed. Carbon deposits were observed on the surfaces of parylene samples ablated in air and nitrogen but not for ablation in vacuum. The deposits could easily be removed using an ultrasonic bath. Scaling exponents for both materials as functions of the number of pulses and for different environments were also evaluated. The most efficient removal of parylene occurs when it is ablated in vacuum. Lack of carbon deposits combined with efficient ablation suggests that processing parylene in vacuum is the most promising method for parylene removal.

Multi-pulse laser ablation thresholds were established for parylene films on gold and for the gold substrates using light with a wavelength of 248 nm and a pulse width of 20 ns. It was determined that the 10-pulse ablation threshold for parylene is 340 mJ/cm^2, while the 300-pulse ablation threshold of gold is 255 mJ/cm^2. This means that at fluences required for quick removal of parylene the gold may be damaged. However, by suitably varying the fluence as a function of the remaining parylene thickness, parylene may be efficiently removed without damaging the gold substrate. Thus, laser ablation has the potential for being an effective method for processing parylene-coated gold and possibly other metals.

Acknowledgements This work was partially supported by grants from the University of Missouri-Research Board, the UMKC Research Board, and NSF Contract Nos. DMR-0605493 and DMR-0923166.

References

1. Hoch HC, Jelinski L, Craighead HG (eds) (2006) Nanofabrication and biosystems. Cambridge University Press, New York
2. Meng E, Tai Y-C (2005) In: 18th IEEE international conference on micro electro mechanical systems, MEMS 2005, Miami, FL, pp 568–571
3. Schmidt EM, Bak MJ, Christensen P (1995) J Neurosci Methods 62:89
4. Sharifi H, Lahiji RR, Lin H-C, Ye PD, Katehi LPB, Mohammadi S (2009) IEEE Trans Adv Packag 32:85
5. Meng E, Li P-Y, Tai Y-C (2008) J Micromech Microeng 18:045004
6. Srinivasan R, Mayne-Banton V (1982) Appl Phys Lett 41:576
7. Lippert T, Dickinson JT (2003) Chem Rev 103:453
8. Esashi M, Minami K, Shoji S (1991) In: Proceedings on the investigation of microstructures, sensors, actuators, machines and robots, MEMS 91, Nara, Japan, pp 39–44
9. Choi Y, Choi S-O, Shafer RH, Allen MG (2005) In: 13th International conference on solid-state sensors, actuators and microsystems (Transducers 05), IEEE, Atlanta, GA, pp 1469–1472
10. Herrault F, Ji C-H, Rajaraman S, Shafer RH, Allen MG (2007) In: International conference on solid-state sensors, actuators and microsystems (Transducers 2007), Lyon, France, pp 513–516
11. Loeb G, Peck R, Martyniuk J (1995) J Neurosci Methods 63:175
12. Rosenfeld A, Campbell EEB (1996) Appl Surf Sci 96–98:439
13. Arenholz E, Heitz J, Wagner M, Bauerle D, Hibst H, Hagenmeyer A (1993) Appl Surf Sci 69:16